

Article

Steady-State Fluorescence and Lifetime Emission Study of pH-Sensitive Probes Based on i-motif Forming Oligonucleotides Single and Double Labeled with Pyrene

Anna Dembska *, Patrycja Rzepecka and Bernard Juskowiak

Adam Mickiewicz University, Faculty of Chemistry, Umultowska 89b, 61-614 Poznan, Poland;
E-Mails: rzepeckap@gmail.com (P.R.); juskowia@amu.edu.pl (B.J.)

* Author to whom correspondence should be addressed; E-Mail: aniojka@amu.edu.pl;
Tel.: +48-61-829-1571; Fax: +48-61-829-1555.

Academic Editor: Igor Medintz

Received: 31 July 2015 / Accepted: 16 September 2015 / Published: 23 September 2015

Abstract: Cytosine-rich nucleic acids undergo pH-stimulated structural transitions leading to formation of an i-motif architecture at an acidic pH. Thus, i-motifs are good foundation for designing simple pH-sensitive fluorescent probes. We report here steady-state and time-resolved fluorescence studies of pyrene-labeled probes based on RET sequence: C₄GC₄GC₄GC₄TA (RET21), AC₄GC₄GC₄GC₄TA (RET21A) and C₄GC₄GC₄GC₄T (RET20). Comparative studies with single- and double-labeled i-motif probes were carried out. For each probe, we have measured fluorescence spectra and decays for emission wavelength of 390 nm over a wide range of pH (from 4.0 to 8.0). Effect of the oligonucleotide sequence and the number of pyrene labels on the spectral characteristics of probes were discussed.

Keywords: fluorescence; lifetime; pyrene; excimer; oligonucleotide probe; i-motif

1. Introduction

The i-motif DNA is formed from cytosine (C)-rich sequences at slightly acidic pH or even neutral pH [1–6]. Such kinds of sequences are often found in the promoter region of proto-oncogenes and human telomeric DNA [4,7–9]. For example, the RET gene encodes a tyrosine kinase that has been connected to the growth of human cancer [8]. Except for their potential role in the gene-regulation

processes, the existence of proteins that specifically bind to C-rich sequences has already been proven [10]. The i-motif structure is constructed as a consequence of the intercalation of two hemiprotonated C-C⁺ base-paired duplexes. Both intra- and intermolecular i-motifs can be created by C-rich oligonucleotides depending mainly on the amount of cytosine tracks and surrounding conditions [6,11,12].

The ability of sequences, including tracks of cytosine, to switch from random coil (“open” state) to folded i-motif (“closed” state) in response to pH decreasing has been explored in biological cycle operating systems [13] and various DNA-nanoactuator machines [14] as well as cellular pH indicators [15–17]. I-motif structures have become important building blocks in DNA nanotechnology, resulting, for example, in fabrication of the one-dimensional nanowires [18] or three-dimensional pillars [19], hydrogels [20], intelligent surfaces [21] and nanopores [22]. On the other hand, studies on fluorescent probes, based on secondary DNA structures (here: i-tetraplexes) [23–27], should bring information necessary to clarify their creation and role in cell biology.

The fluorescence decay curves in biological systems are often difficult to interpret due to factors such as the dynamics of the system in the ps–ns scale, many conformational states, relaxation processes or the heterogeneous environment. Moreover, in the case of biological systems, it seems most reasonable to perform the analysis of lifetime distributions and, especially, to calculate the amplitude-weighted average lifetime [28].

The pH-dependence architecture of i-motifs makes them a good foundation for designing simple fluorescent probes for pH monitoring. Therefore, we previously proved that pyrene-modified i-motifs folding c-myc-derived sequences emit fluorescence with intensity decreasing upon pH lowering [29]. In the latter case, we supposed that the long loop present in c-myc-based i-motif is somehow responsible for lack of excimer emission.

As an extension of this project, we performed steady-state fluorescence and lifetime emission studies of probes based on RET sequence: C₄GC₄GC₄GC₄TA (RET21), AC₄GC₄GC₄GC₄TA (RET21A) [30] and C₄GC₄GC₄GC₄T (RET20) [30]. Contrary to c-myc, RET sequence forming i-motif is classified to class I with short loop [9]. Comparative studies with single- and double-labeled i-motifs were carried out (Table 1). For each probe, we have measured fluorescence decays for emission wavelength of 390 nm over a wide range of pH (from 4.0 to 8.0). All decays of investigated systems were analyzed using multi-exponential model, and the amplitude-weighted as well as the fractional-weighted average lifetimes for every probe were calculated.

Table 1. Oligonucleotide probes.

Probe	Oligonucleotide	5' label	3' label
Py-RET21A-Py	d(ACCCCGCCCCGCCCCGCCCTA)	Pyrene	Pyrene
Py-RET21A	d(ACCCCGCCCCGCCCCGCCCTA)	Pyrene	-----
Py-RET21-Py	d(CCCCGCCCCGCCCCGCCCTA)	Pyrene	Pyrene
Py-RET21	d(CCCCGCCCCGCCCCGCCCTA)	Pyrene	-----
RET21-Py	d(CCCCGCCCCGCCCCGCCCTA)	-----	Pyrene
Py-RET20-Py	d(CCCCGCCCCGCCCCGCCCT)	Pyrene	Pyrene
RET20-Py	d(CCCCGCCCCGCCCCGCCCT)	-----	Pyrene

2. Experimental Section

2.1. Materials

The oligonucleotides: d(C₄GC₄GC₄GC₄TA) (RET21), d(AC₄GC₄GC₄GC₄TA) (RET21A) and d(C₄GC₄GC₄GC₄T) (RET20) with modifications called 5' C6-Aminolink and/or 3' C7-Aminolink were purchased from Generi Biotech (Czech Republic). All oligonucleotides were purified by means of high performance liquid chromatography (HPLC). All probes (see Table 1) were synthesized according to the procedure described by Kierzek *et al.* [31] in the reaction of coupling between amino-functionalized DNA and pyrene activated ester. Each reaction was carried out overnight in NaHCO₃, pH 8.5. All synthesized products were purified by means of high performance liquid chromatography (HPLC) on C18 reverse phase column. The identities of products were confirmed by Matrix Assisted Laser Desorption/Ionization Time of Flight Mass Spectrometry (MALDI-TOF MS) analysis performed in Centre of Molecular and Macromolecular Studies in Lodz, Poland. Other reagents were of analytical grade purity and were used as received. The buffer used in the work was 10 mM Tris adjusted to desired pH by acetic acid. High-purity water (Polwater, Poland) was used throughout. The concentrations of the strands were determined by UV absorbance at 260 nm, measured at a high temperature (above 85 °C), assuming the molar extinction coefficients of 7400 M⁻¹cm⁻¹ for cytosine; 15,400 M⁻¹cm⁻¹ for adenine; 8700 M⁻¹cm⁻¹ for thymine; 11,500 M⁻¹cm⁻¹ for guanine and 16,500 M⁻¹cm⁻¹ for pyrene [32]. Before the spectral measurements, the 1 μM solutions of every probe in appropriate buffers were annealed by being heated to 90 °C, then left to slowly cooling to room temperature and kept at 4 °C overnight.

2.2. Circular Dichroism (CD) Spectroscopy

CD spectra were recorded on a Jasco J-810 spectropolarimeter at room temperature. Each measurement was the average of four repeated scans recorded from 230 to 400 or 420 nm with a 10 mm quartz cell at a scan speed of 200 nm/min. The scan of the corresponding buffer solution was subtracted from the average scan for each sample.

2.3. Fluorescence Spectroscopy

Steady-state fluorescence measurements were carried out on a Cary Eclipse spectrofluorimeter (Agilent Technologies) with 5 nm excitation and 10 nm emission slits and were carried out using 0.2 × 1 cm quartz cuvettes, containing 1 mL of solution. Fluorescence emission spectra were collected from 370 to 620 nm with excitation at 340 nm. All emission spectra were uncorrected.

Fluorescence lifetime measurements were done using a time correlated single photon counting (TCSPC) by means of Fluo-time 300 fluorometer (PicoQuant, Germany). The samples were excited at 330 nm using PLS(330) LED diode and the photons were counting until at least 10,000 counts were collected at the maxima of the fluorescence decay histograms. The fluorescence intensity was monitored at 390 nm characteristic of pyrene monomer emission unless otherwise stated. The raw data were analyzed by a multi-exponential model with reconvolution of the instrument response function (IRF) with using FluoFit v4.5 software (PicoQuant). The software automatically calculated the

amplitude-weighted as well as the fractional-weighted average lifetimes. The quality of the fit was judged from the χ^2 values ($\chi^2 \leq 1.5$) and random distribution of weighted residuals.

3. Results and Discussion

3.1. Design of Pyrene-Modified i-Motifs Based on RET Sequence

The modified oligonucleotides used in presented studies are collected in Table 1. All sequences contain 20-mer part being, indeed, found in RET proto-oncogene and proved to self-assemble into intramolecular i-motif in acidic pH [8].

The working principle of dual-pyrenyl-end-labeled i-motifs is shown in Figure 1. The proposed i-motif based sensors would give analytical response to pH lowering in monomer/excimer mode (EMS). Pyrene and its derivatives are known to exhibit excimer fluorescence induced by stacking interactions between at least two aromatic rings [33,34]. In our case, the formation of i-motif should bring on stacking interactions between fluorophores (pyrene/pyrene) and produce excimer emission with maximum around 480 nm. One of our concerns was that the difference in the length of free ends hanging after i-motif formation could stand in the way of pyrene residues meeting in the desired orientation. Therefore, we designed three probes possessing different amount of flanking bases (Figure 2).

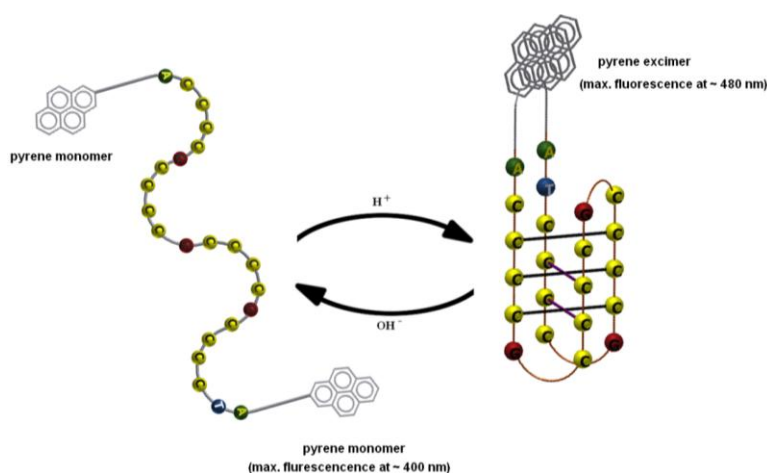


Figure 1. The assumed working idea of the pH-sensitive probe based on i-motif forming oligonucleotide double labeled with pyrene.

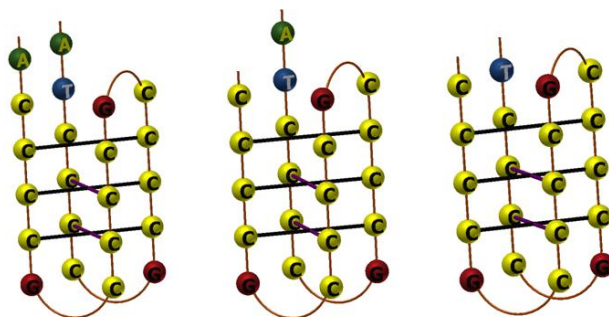


Figure 2. The schematic representation of i-motifs formed by C-rich sequences: (a) AC₄GC₄GC₄GC₄TA (RET21A); (b) C₄GC₄GC₄GC₄TA (RET21); and (c) C₄GC₄GC₄GC₄T (RET20).

3.2. Formation of *i*-Motifs by Pyrene-Modified RET Sequences

Circular dichroism (CD) spectra of nucleic acids in solution provide reliable information on their conformations [35]. For all probes, we obtained CD spectra in the wavelength region 220–400 nm. Examples of experimental curves for Py-RET21A-Py, Py-RET20-Py and Py-RET21-Py in acidic, neutral and slightly basic pH are shown in Figure 3 and Figure S1 (in Supplementary material). In acidic pH, all the spectra exhibited positive Cotton effect with peak at 288 and negative Cotton effect with weak peak at 262 nm. These two bands are characteristic for an *i*-motif secondary structure, however the exact position of these bands is dependent on the nature of bases located at the loops [12]. Furthermore, we could not detect an induced CD signal at 340 nm in any case. These results suggest that pyrene residues do not strongly interact with the *i*-motif. CD spectra proved that attaching pyrene tags did not affect folding properties of *i*-motif-forming oligonucleotides. This conclusion is supported by UV absorption spectra of analyzed systems measured in wide range pH (from pH 4.0 till 8.0) as well as temperatures (from 20 °C till 85 °C) (data not shown).

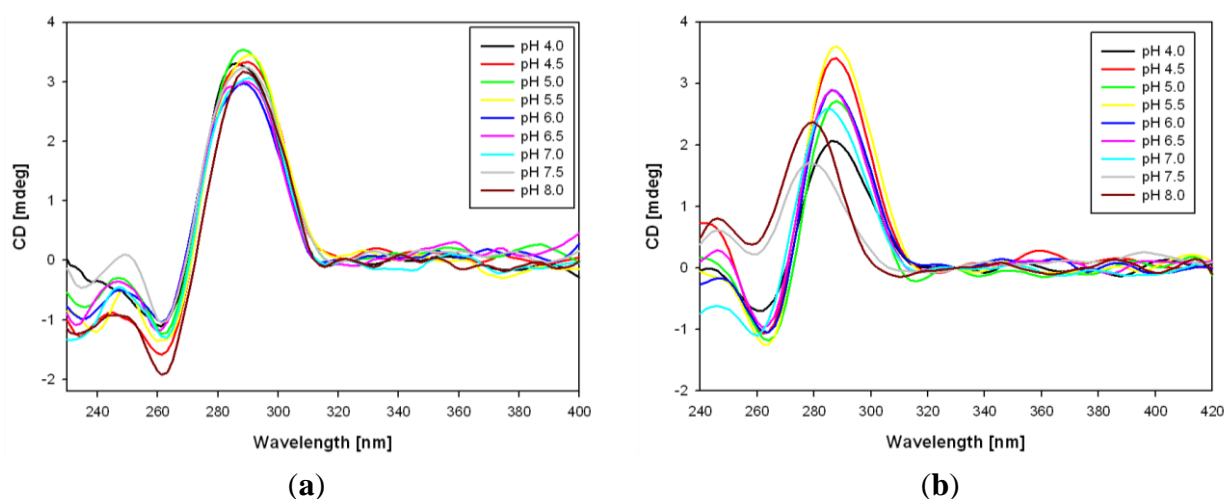


Figure 3. The circular dichroism (CD) spectra of probes double labeled with pyrene recorded at different pH values: (a) Py-RET21A-Py and (b) Py-RET20-Py.

There is almost no change in the localization of the CD minima and maxima up to pH 7.0 for Py-RET20-Py and to pH 8.0 for Py-RET21A-Py. For the latter, we were not able to indicate pH-transition midpoint. The transitional pH for Py-RET20-Py is located between 7.0 and 7.5 as the positive maximum begins to shift toward 277 nm at pH 7.0 (Figure 3b). *i*-motifs formed by dual-pyrene functionalized C-rich oligonucleotides are more stable than unlabeled ones, which is in good agreement with our previous work [29].

3.3. Fluorescence Properties of Pyrene-Modified *i*-Motifs Based on RET Sequence

Figure 4 shows fluorescence emission spectra of Py-RET21A-Py, Py-RET21-Py and Py-RET20-Py in buffers at pH range 4.0–8.0 (with excitation at 340 nm). In all cases, only single emission band at *ca.* 390 nm with vibrational structure characteristic of the pyrene monomer fluorescence is observed [36]. The absence of excimer emission for *i*-motif forming oligonucleotides double labeled with pyrene probe was not due to the lack of *i*-motif architecture since attachment of pyrene moieties

does not affect formation of i-motif structure as it was evidenced by CD measurements (Figures 3 and S1 in Supplementary material).

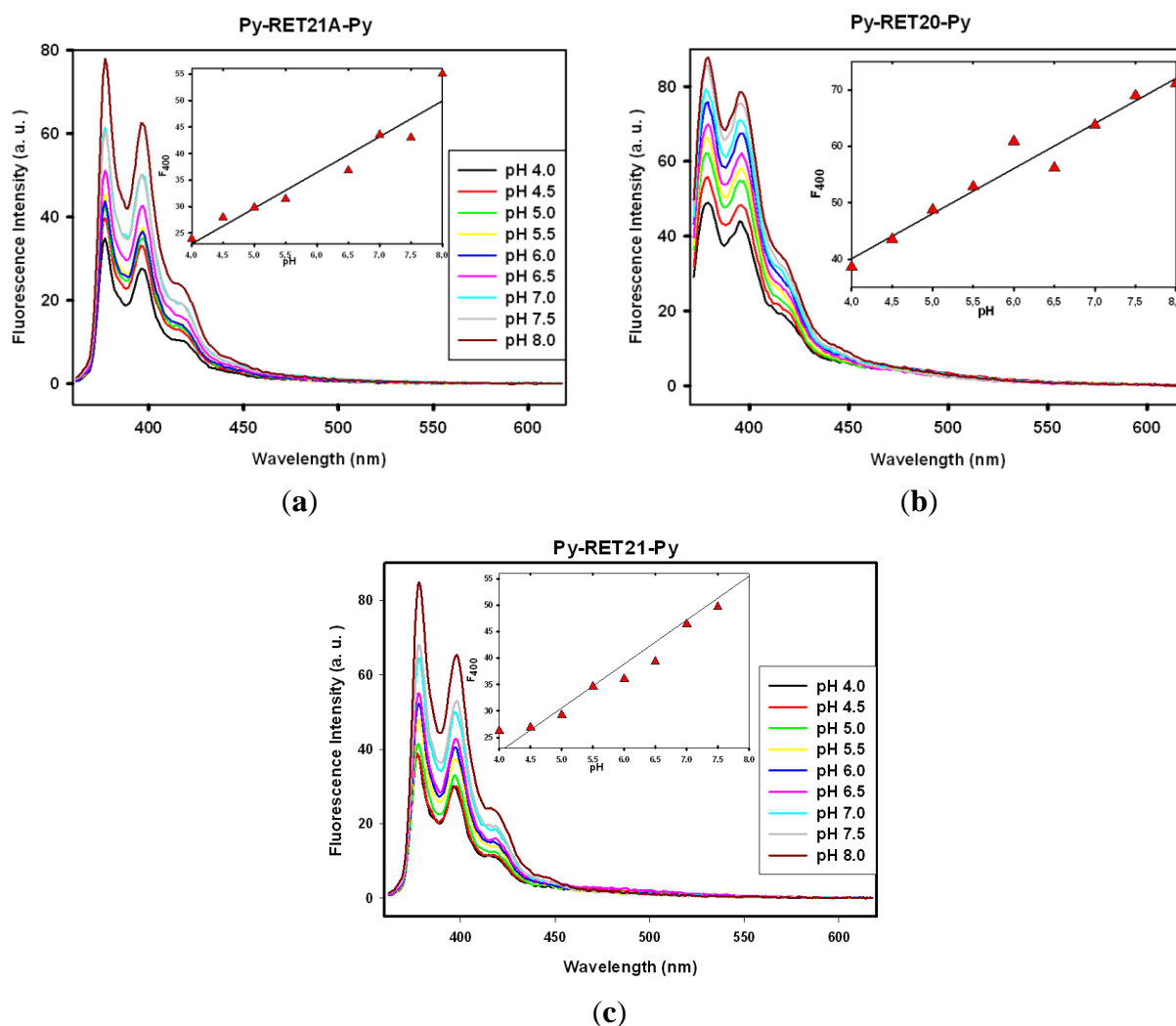


Figure 4. The fluorescence spectra of probes double labeled with pyrene measured at different pH values (1 μ M probe in 10 mM Tris-acetate buffers; excited at 340 nm) with insert showing changes in fluorescence intensity at 400 nm *versus* pH: (a) Py-RET21A-Py; (b) Py-RET20-Py; and (c) Py-RET21-Py.

The presence of flanking bases not engaged into i-motif core was insufficient to help pyrene tags to create fluorescent dimer. These results are consistent with the focus of our previous studies on attempts to examine the capability of c-myc derived sequences double-labeled with pyrene [29]. In the latter case, we supposed that the long loop present in c-myc based i-motif is somehow responsible for lack of excimer emission. However, this hypothesis can be excluded in case of RET sequence forming i-motif, which is classified to class I with short loop [9].

Interestingly, mono-pyrene labeled systems show much less pronounced effect of pH on fluorescence intensities comparing with double-pyrene labeled systems (compare inserts in Figure 4 with inserts in Figure S2 in Supplementary material). For example, intensity of monomer fluorescence band at 400 nm decreased almost by 40% upon pH lowering from 8.0 till 4.5 for Py-RET20-Py,

whereas it was reduced only by 5% in the case of RET20-Py. These results may indicate that even if we do not observe pyrene excimer fluorescence in the case of dual-pyrene labeled i-motifs, the pyrene tags interact with one another forming non-fluorescent pyrene dimers (GSD—Ground State Dimer). To understand the lack of long-wave emission in spectra of dual-pyrenyl-end-labeled i-motifs, a comparative fluorescence lifetime study with single-labeled i-motifs were carried out.

3.4. Lifetime Study of Pyrene-Modified i-Motifs Based on RET Sequence

Excitation wavelength in lifetime experiments was set at 330 nm (pyrene absorption band) and the excited state kinetics was monitored at 390 nm (pyrene monomer fluorescence). The background emission was significantly lower than emission arising from the pyrene-labeled probes and was neglected in further study. We also measured time profiles for Py-RET21A-Py, Py-RET21-Py and Py-RET20-Py at 480 nm (pyrene excimer fluorescence). Similarity between decay traces recorded at 390 and 480 nm suggested that an additional long-wavelength emission was absent here, in good agreement with the lack of excimer emission band in their steady-state fluorescence spectra. Moreover, results obtained for 390 nm appeared to be more reliable due to the higher signal-to-noise ratio at this wavelength.

Examples of experimental decays collected at 390 nm for Py-RET21A-Py, Py-RET21-Py and Py-RET20-Py and at 480 nm for Py-RET21-Py in acidic, neutral and slightly basic pH are shown in Figure 5. For the analysis of decay curves of i-motif forming oligonucleotides single and double labeled with pyrene, we used multi-exponential model even though the systems contain only one type of fluorescent tag (here: pyrene). All decays of investigated systems could be characterized by a di-exponential rate provided that the amplitude of the scattered light contribution is taken into account. Considering the fact that the traditional multi-exponential model is actually not proper for interpretation decays of fluorescence intensity in biological systems [37], in our discussion we focus on average lifetimes calculated for each probe (Figure 6 and Table S1 in Supplementary material). Unfortunately, we did not observed any linear relationship between pH and average lifetimes calculated for probes double labeled with pyrene as we expected on the basis on their steady-states spectra (Figure 4). The values of the amplitude-weighted average lifetimes obtained for Py-RET21A-Py (*ca.* 10 ns) are about twice times shorter than for Py-RET21-Py and Py-RET20-Py (*ca.* 20–35 ns). What is more, the average lifetimes calculated for Py-RET21A-Py are almost the same in the whole range of pH (from 4.0 to 8.0). These results are consistent with CD spectra measurements showing that i-motif formed by Py-RET21A-Py is stabilized in the same way at pH 4.0 and pH 8.0.

In all cases, the calculated amplitude-weighted pyrene fluorescence average lifetimes, $\langle\tau\rangle$ (Figure 6 and Table S1 in Supplementary material) are quenched in comparison with free pyrenebutanoic acid (PBA). The PBA lifetime amounts 90 ns in non-deaerated Tris-acetate buffer measured by us in the same experimental conditions. The observed quenching can be caused by pyrene/nucleobase stacking interactions and/or by electron transfer. It is known that attachment of the pyrene moiety to DNA oligonucleotide probe results in substantial decrease in fluorescence quantum yield, which is ascribed to the electron transfer (ET) between pyrene and DNA nucleobases (except for adenine [38]). Recently, Majima *et al.* proved that electron transfer in i-motif DNA is even more efficient than in the duplex DNA due to the compact structure of i-motif [39].

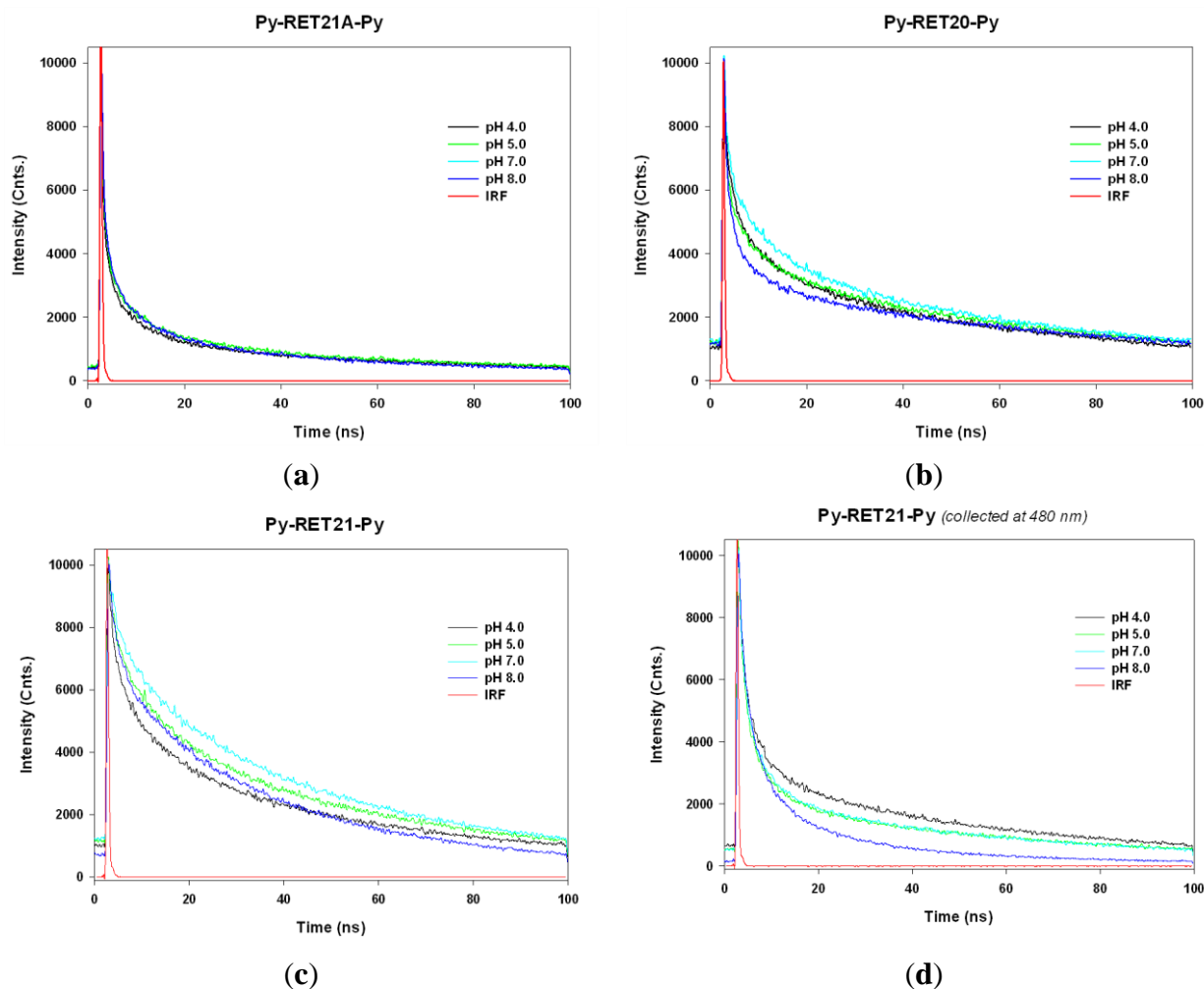


Figure 5. The fluorescence intensity decays for probes double labeled with pyrene; collected at 390 nm (a–c) and 480 nm (d) in different pH values (10 mM Tris-acetate buffers): (a) Py-RET21A-Py; (b) Py-RET20-Py; and (c,d) Py-RET21-Py.

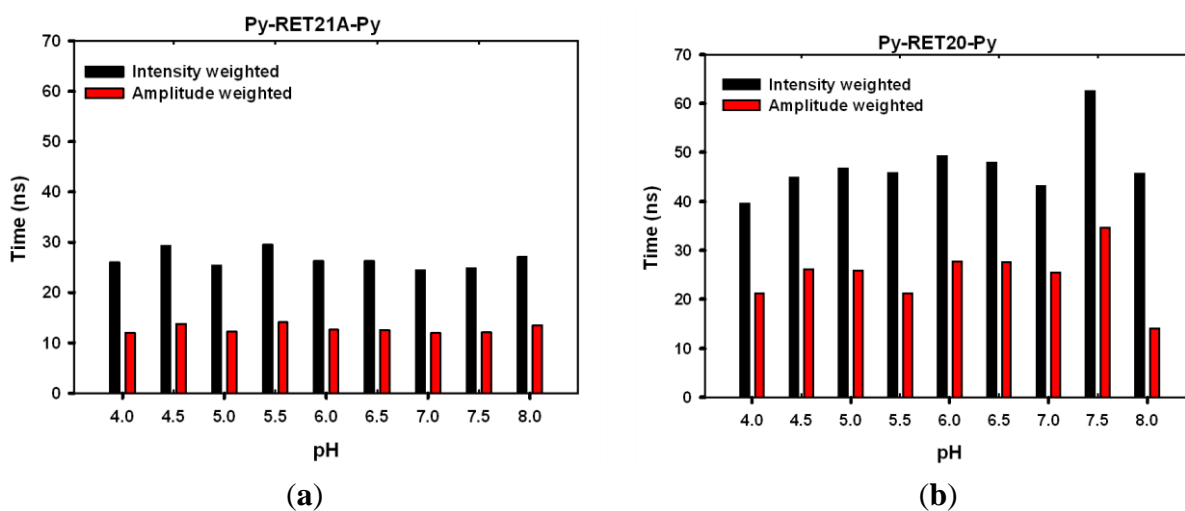


Figure 6. Cont.

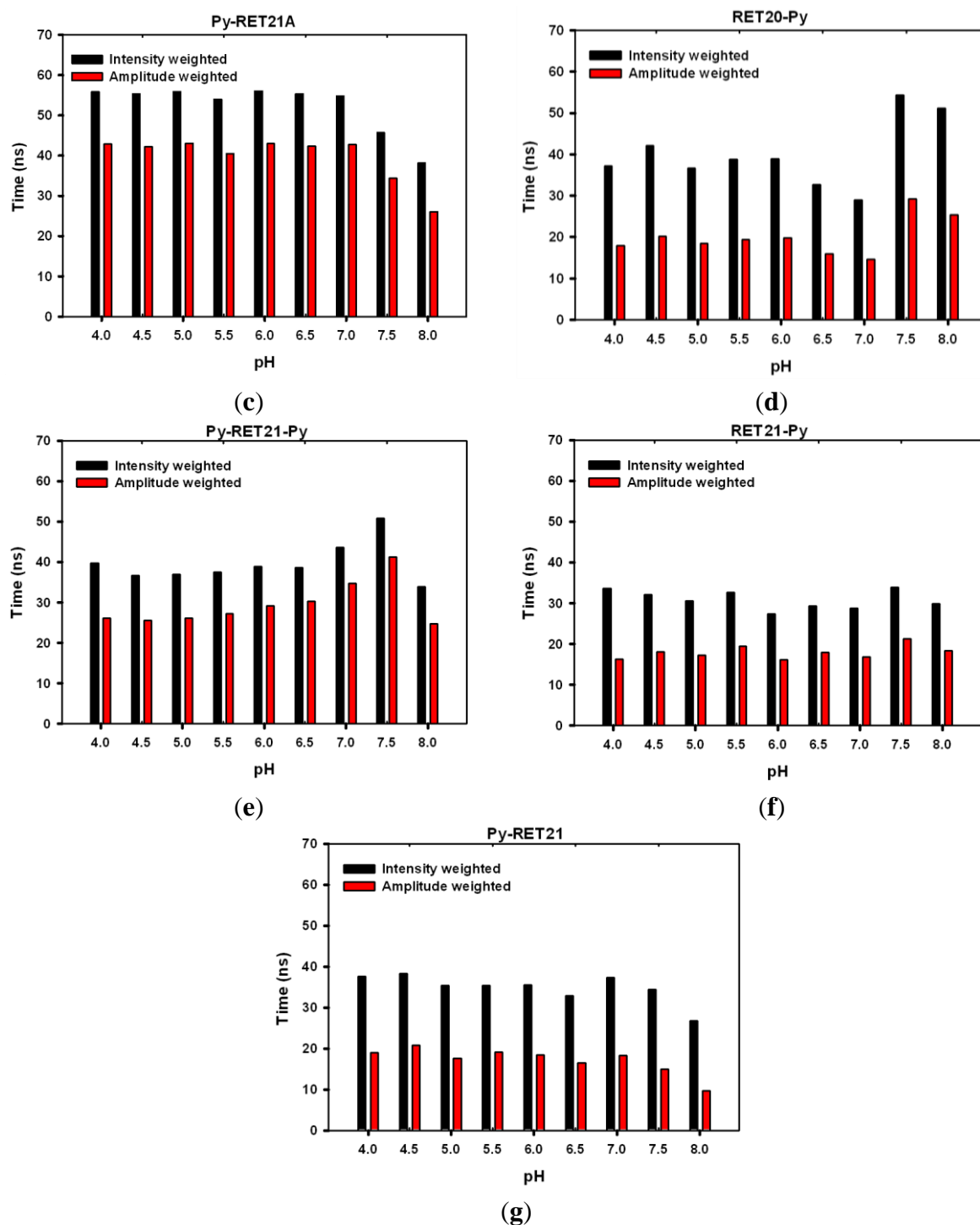


Figure 6. The diagrams illustrating distribution of intensity weighted and amplitude weighted lifetimes of dual- and mono-pyrene labeled probes: (a) Py-RET21A-Py; (b) Py-RET20-Py; (c) Py-RET21A; (d) RET20-Py (e) Py-RET21-Py; (f) RET21-Py; and (g) Py-RET21.

The calculated amplitude-weighted pyrene fluorescence average lifetimes, $\langle\tau\rangle$, values for Py-RET21A (ca. 40 ns) are about 75% higher than those calculated for Py-RET21A-Py. The additional adenine at 5' end of RET21A contributed to increasing of $\langle\tau\rangle$ in case of Py-RET21A and decreasing of $\langle\tau\rangle$ in case of Py-RET21A-Py. It seems probable that the dramatic shortening of $\langle\tau\rangle$ for Py-RET21A-Py is

caused by forming GSD, which is excluded in the case of Py-RETA21. The question is why amplitude average lifetimes of Py-RET21A are 2–4 times longer than those for other investigated mono-pyrene labeled systems (Figure 6 and Table S1 in Supplementary material). Considering topology of RET21A (Figure 2), one can easily find out that pyrene residue at the 5' end of Py-RET21A has adenine as a neighbor and A is an opposite base. Adenine can be considered a “safe” neighbor in terms of ET between pyrene and nucleobase [38]. Contrary to RET21A, pyrene residues attached to 5' end of RET21 or 3' end of RET20 as well as RET21 are expected to interact with cytosine not involved in forming i-motif skeleton, as cytosine is next to or opposite to pyrene, respectively. Cytosine as well as thymine bases are acceptors for ET from pyrene [38]. It is worth noting that the calculated amplitude-weighted average lifetimes for Py-RET21-Py and Py-RET20-Py and their mono-labeled analogues (Py-RET21, RET21-Py and RET20-Py) are almost identical (*ca.* 20–35 ns), indicating that similar mechanism is involved in quenching pyrene monomer fluorescence of these probes.

Summarizing, additional flanking bases in designed dual-pyrene functionalized i-motif forming probes not engaged in the i-motif core were not sufficient to help pyrene tags to create fluorescent dimer (excimer) and to prevent them from efficient electron transfer quenching.

4. Conclusions

We assumed that the i-motif architecture would be suitable to help pyrene tags, attached to both ends of C-rich oligomers, to form sandwich structure emitting excimer fluorescence. However, the steady-state fluorescent measurements indicate that designed probes based on RET sequence exhibited only pyrene monomer fluorescence in the “open” state (intense pyrene monomer fluorescence) at alkaline pH as well as in the folded conformation—“closed” state (quenched pyrene monomer fluorescence)—at acidic pH. Additional flanking bases not engaged into i-motif core were also not enough to help pyrene tags to form fluorescent dimer. The time profiles obtained for probes mono as well double labeled with pyrene were fitted to di-exponential decays when amplitude of the scattered light contribution was taken into account. Moreover, we did not observe any linear relationship between pH and average lifetimes calculated for all samples. The analysis of monomer emission data indicated that quenching of pyrene excited state could be attributed to interactions with nucleobases and/or with second pyrene molecule. The more detailed studies, such as nanosecond time-resolved laser flash photolysis and/or transient absorption measurements, are needed to fully explain and understand the mechanism of fluorescence quenching of pyrene emission by i-motif forming oligonucleotides.

The presented results confirmed our earlier studies [29] with different intramolecular i-motif sequences labeled with pyrene devoted to develop pH indicators working in an excimer/monomer-switching mode. The final conclusion is that elongation of i-motifs ends leading to formation a duplex blunt end should enable arrangement of pyrene moieties that promote formation of fluorescent excimer. This idea has been further developed by us [40].

Acknowledgments

This research was financially supported by the Research Grant No. N N204 220040 from the National Science Center of Poland.

Author Contributions

Conceived and designed the experiments: A.D. and B.J. Performed the experiments: A.D and P.R. Analyzed the data: A.D. Wrote and edited the manuscript: A.D. Supervised the project and edited the manuscript: B.J.

Conflicts of Interest

The authors declare no conflict of interest.

References and Notes

1. Gehring, K.; Leroy, J.L.; Gueron, M. A tetrameric DNA structure with protonated cytosine-cytosine base pairs. *Nature* **1993**, *363*, 561–565.
2. Manzini, G.; Yathindra, N.; Xodo, L.E. Evidence for intramolecularly folded i-DNA structures in biologically relevant CCC-repeat sequences. *Nucleic Acids Res.* **1994**, *22*, 4634–4640.
3. Mergny, J.-J.; Lacroix, L.; Han, X.G.; Leroy, J.L.; Helene C. Intramolecular folding of pyrimidine oligodeoxynucleotides into an i-DNA motif. *J. Am. Chem. Soc.* **1995**, *117*, 8887–8898.
4. Kumar, P.; Verma, A.; Maiti, S.; Gargallo, R.; Chowdhury, S. Tetraplex DNA Transitions within the human c-myc promoter detected by multivariate curve resolution of fluorescence resonance energy transfer. *Biochemistry* **2005**, *44*, 16426–16434.
5. Zhou, J.; Wei, C.; Jia, G.; Wang, X.; Feng, Z.; Li, C. Formation of i-motif structure at neutral and slightly alkaline pH. *Mol. Biosyst.* **2010**, *6*, 580–586.
6. Gueron, M.; Leroy, J.-L. The i-motif in nucleic acids. *Curr. Opin. Struct. Biol.* **2000**, *10*, 326–331.
7. Leroy, J.L.; Gueron, M.; Mergny, J.L.; Helene, C. Intramolecular folding of a fragment of the cytosine-rich strand of telomeric DNA into an i-motif. *Nucleic Acids Res.* **1994**, *22*, 1600–1606.
8. Guo, K.; Pourpak, A.; Beetz-Rogers, K.; Gokhale, V.; Sun, D.; Hurley, L.H. Formation of pseudosymmetrical G-quadruplex and i-motif structures in the proximal promoter region of the RET oncogene. *J. Am. Chem. Soc.* **2007**, *129*, 10220–10228.
9. Brooks, T.A.; Kendrick, S.; Hurley, L. Making sense of G-quadruplex and i-motif functions in oncogene promoters. *FEBS J.* **2010**, *277*, 3459–3469.
10. Marisch, E.; Xodo, L.E.; Manzini, G. Widespread presence in mammals and high binding specificity of a nuclear protein that recognise the single-stranded telomeric motif (CCCTAA)_n. *Eur. J. Biochem.* **1998**, *258*, 93–99.
11. Day, H.A.; Pavlou, P.; Waller, Z.A.E. i-motif DNA: Structure, stability and targeting with ligands, *Biorg. Med. Chem.* **2014**, *22*, 4407–4418.
12. Benabou, S.; Avino, A.; Eritja, R.; Gonzalez, C.; Gargallo, R. Fundamental aspects of the nucleic acid i-motif structures. *RSC Adv.* **2014**, *4*, 26956–26980.
13. Liedl, T.; Simmel, F.C. Switching the Conformation of a DNA Molecule with a Chemical Oscillator. *Nano Lett.* **2005**, *5*, 1894–1898.
14. Liu, D.; Bruckbauer, A.; Abell, C.; Balasubramanian, S.; Kang, D.J.; Klenerman, D.; Zhou, D. A reversible pH-driven DNA nanoswitch array. *J. Am. Chem. Soc.* **2006**, *128*, 2067–2071.

15. Modi, S.; Swetha, M.G.; Goswami, D.; Gupta, G.D.; Mayor, S.; Krishnan, Y. A DNA nanomachine that maps spatial and temporal pH changes in living cells. *Nat. Nanotechnol.* **2009**, *4*, 325–330.
16. Surana, S.; Bhatt, J.M.; Koushika, S.P.; Krishnan, Y. An autonomous DNA nanomachine maps spatial and temporal pH changes in a multicellular living organism. *Nat. Commun.* **2011**, *2*, 339.
17. Huang, J.; He, Y.; Yang, X.; Wang, K.; Ying, L.; Quan, K.; Yanga, Y.; Yin, B. I-motif-based nano-flares for sensing pH changes in live cells. *Chem. Commun.* **2014**, *50*, 15768–15771.
18. Ghodke, H.B.; Krishnan, R.; Vignesh, K.; Kumar, G.; Narayana, C.; Krishnan, Y. The i-tetraplex building block: Rational design and controlled fabrication of robust 1D DNA scaffolds through non-Watson-Crick interactions. *Angew. Chem. Int. Ed.* **2007**, *119*, 2700–2703.
19. Yang, Y.; Zhou, C.; Zhang, T.; Cheng, E.; Yang, Z.; Liu, D. DNA pillars constructed from an i-motif stem and duplex branches. *Small* **2012**, *8*, 552–556.
20. Cheng, E.; Xing, Y.; Chen, P.; Yang, Y.; Sun, Y.; Zhou, D.; Xu, L.; Fan, Q.; Liu, D. A pH-Triggered, Fast-Responding DNA Hydrogel. *Angew. Chem. Int. Ed.* **2009**, *48*, 7660–7663.
21. Wang, S.; Liu, H.; Liu, D.; Ma, X.; Fang, X.; Jiang, L. Enthalpy driven three-state switching of a superhydrophilic/superhydrophobic surface. *Angew. Chem. Int. Ed.* **2007**, *46*, 3915–3917.
22. Xia, F.; Guo, W.; Mao, Y.; Hou, X.; Xue, J.; Xia, H.; Wang, L.; Song, Y.; Ji, H.; Ouyang, Q. Gating of single synthetic nanopores by proton-driven DNA molecular motors. *J. Am. Chem. Soc.* **2008**, *130*, 8345–8350.
23. Mergny, J.L. Fluorescence energy transfer as a probe for tetraplex formation: The i-motif. *Biochemistry* **1999**, *38*, 1573–1581.
24. Lee, I.J.; Park, M.; Joo, T.; Kim, B.H. Using fluorescence changes of F1U units at terminal and mid-loop positions to probe i-motif structures. *Mol. Biosyst.* **2012**, *8*, 486–490.
25. Lee, I.J.; Kim, B.H. Monitoring i-motif transitions through the exciplex emission of a fluorescent probe incorporating two (Py)A units. *Chem. Commun.* **2012**, *48*, 2074–2076.
26. El-Sayed, A.A.; Pedersen, E.B.; Khaireldin, N.A. Studying the influence of the pyrene intercalator TINA on the stability of DNA i-motifs. *Nucleosides Nucleotides Nucleic Acids* **2012**, *31*, 872–879.
27. Lee, I.J.; Patil, S.P.; Fhayli, K.; Alsaiaia, S.; Khashab, N.M. Probing structural changes of self assembled i-motif DNA. *Chem. Commun.* **2015**, *51*, 3747–3749.
28. Dembska, A.; Juskowiak, B. The Fluorescence Properties and Lifetime Study of G-quadruplexes Single- and Double-labeled with Pyrene. *J. Fluoresc.* **2010**, *20*, 1029–1035.
29. Dembska, A.; Rzepecka, P.; Juskowiak, B. Spectroscopic Characterization of i-motif Forming c-myc Derived Sequences Double-Labeled with Pyrene. *J. Fluoresc.* **2013**, *23*, 807–812.
30. Dembska, A.; Rzepecka, P.; Juskowiak, B. Steady-state fluorescence and lifetime emission study of i-motifs single and double labeled with pyrene. Markoš, J., Ed.; In Proceedings of the 41th International Conference of Slovak Society of Chemical Engineering, Tatranské Matliare, Slovakia, 26–30 May 2014; pp. 697–703.
31. Kierzek, R.; Li, Y.; Turner, D.H.; Bevilacqua P.C. 5'-Amino Pyrene Provides a Sensitive, Nonperturbing Fluorescent Probe of RNA Secondary and Tertiary Structure Formation. *J. Am. Chem. Soc.* **1993**, *115*, 4985–4992.

32. Fasman, G.D. (Ed.) *Handbook of Biochemistry and Molecular Biology, Volume 1: Nucleic Acids*, 3rd ed.; CRC Press: Boca Raton, FL, USA, 1975.
33. Birks, J.B.; Dyson, D.J.; Munro, I.H. “Excimer” Fluorescence. II. Lifetime Studies of Pyrene Solutions. *Proc. R. Soc. Lond.* **1963**, *275*, 575–588.
34. Turro, N.J. *Modern Molecular Photochemistry*; Benjamin/Cummings: Menlo Park, CA, USA, 1978; pp. 141–143.
35. Kypr, J.; Kejnovska, I.; Renciuik, D.; Vorlickova, M. Circular dichroism and conformational polymorphism of DNA. *Nucleic Acids Res.* **2009**, *37*, 1713–1725.
36. Every experiment was repeated 3 to 5 times; very weak fluorescence emission band at 480 nm occurred in some measurements.
37. Kierdaszuk, B. From discrete multi-exponential model to lifetime distribution model and power law fluorescence decay function. *Spectroscopy* **2010**, *24*, 399–407.
38. Manoharan, M.; Tivel, K.L.I.; Zhao, M.; Nafisi, K.; Netzl, T.L. Base-Sequence Dependence of Emission Lifetimes for DNA Oligomers and Duplexes Covalently Labeled with Pyrene: Relative Electron-Transfer Quenching Efficiencies of A, G, C and T Nucleosides toward Pyrene. *J. Phys. Chem. B* **1995**, *99*, 17461–17472.
39. Choi, J.; Tanaka, A.; Cho, D.W.; Fujitsuka, M.; Majima, T. Efficient electron transfer in i-Motif DNA with a Tetraplex Structure. *Angew. Chem. Int. Ed.* **2013**, *52*, 12937–12941.
40. Dembska, A.; Juskowiak, B. Pyrene functionalized molecular beacon with pH-sensitive i-motif in a loop. *SAA* **2015**, *150*, 928–933.

© 2015 by the authors; licensee MDPI, Basel, Switzerland. This article is an open access article distributed under the terms and conditions of the Creative Commons Attribution license (<http://creativecommons.org/licenses/by/4.0/>).